# Effects of CO, H$_2$ and C$_3$H$_6$ on Cu-SSZ-13 catalyzed NH$_3$-SCR

Yang Zheng, Michael P. Harold*, Dan Luss*

Department of Chemical & Biomolecular Engineering, University of Houston, Houston, TX 77204, USA
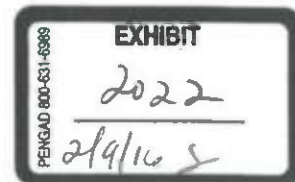
ABSTRACT

We investigated the steady-state and transient effects of reductants (CO, H$_2$ and C$_3$H$_6$) on NO$_2$ reduction, NH$_3$-SCR (selective catalytic reduction), NH$_3$ adsorption and oxidation, and N$_2$O production on a Cu-SSZ-13 monolithic catalyst. The three reductants affect to different extents the standard SCR (NO + NH$_3$ + O$_2$), fast SCR (NO + NH$_3$ + NO$_2$), and slow SCR (NH$_3$ + NO$_2$). This study underscores the importance of accounting for the impact of reducing agents on conventional NH$_3$-SCR reaction mechanism when SCR catalyst is subjected to either rich regeneration of integrated systems (LNT + SCR, SCR on DPF) or cold-start. Propylene is most effective in promoting NO$_2$ reduction to NO by formation of organic intermediates. CO effectively reduces nitrates to nitrites that then react with NO$_2$, releasing NO. H$_2$ can follow a similar pathway as CO but is less effective. In addition, H$_2$ can also enable a H$_2$-based SCR pathway through the reduction of Cu cations to Cu$^0$ which then catalyze the NOx reduction. This pathway is particularly evident at high temperatures and low O$_2$ levels. As for NH$_3$-SCR reactions, propylene competes with NH$_3$ for adsorbed NO$_2$, which generates NO and thus increases the NO/NOx ratio. This leads to the dominance of either fast or standard SCR for a slow SCR (NH$_3$ + NO$_2$) feed condition when C$_3$H$_6$ is present. CO has only a minor effect on both standard and fast SCR but a promoting effect on slow SCR. The ineffective reduction of NO$_2$ to NO by H$_2$ at low temperature ($T < 250$ C) results in a negligible effect on slow SCR. In contrast to steady-state operation, lean/rich cycling enhances cycle-averaged NOx conversion for each of the NH$_3$-SCR reactions when adding either C$_3$H$_6$ or a CO + H$_2$ mixture in the rich phase. A decreased N$_2$O generation rate from the slow SCR reaction is observed when any of the three reductants are present due in part to their reaction with ammonium nitrates.

© 2015 Elsevier B.V. All rights reserved.

## 1. Introduction

Lean-burn gasoline and diesel engines achieve a higher fuel economy than stoichiometric gasoline engines. Their use will enable vehicle manufacturers to meet the stringent 2017–2025 US EPA greenhouse gas and NHTSA (National Highway Traffic Safety Administration) fuel economy standards [1]. A major challenge of lean-burn application is the reduction of nitrogen oxides (NOx; NO + NO$_2$) in a net oxidizing environment. Ever-tightening Tier 3 and LEV III emission regulations exacerbate this technological challenge [2]. Two commercialized deNOx technologies that meet the current emission standards are NOx storage and reduction (NSR) and selective catalytic reduction (SCR). The SCR technology reduces NOx to N$_2$ by reaction over vanadium-based or transition metal exchanged zeolite catalysts with NH$_3$ generated from urea hydrolysis. SCR is the leading deNOx solution for mid- or heavy-duty vehicles and can achieve over 95% deNOx efficiency at practically relevant space velocities. It requires an onboard urea storage and delivery system with a minimum urea dosing temperature requirement of ~200 C. This limits its function during cold-start or low-load conditions. For light-duty lean-burn vehicles, NSR is preferred. It involves the storage of NOx on a lean NOx trap (LNT) catalyst under lean conditions, followed by a short, rich regeneration by a mixture of CO, H$_2$ and hydrocarbons (HC) [3]. The LNT catalyst requires precious group metals (PGM) to achieve a high NOx conversion. However, it is not as selective as SCR, producing byproducts such as N$_2$O and NH$_3$.

The integration of SCR with NSR (or equivalently LNT) has aroused much interest [4–6]. One example is the LNT + passive SCR system wherein the SCR catalyst utilizes NH$_3$ produced by the upstream LNT during rich purges to achieve incremental NOx reduction. This system lowers the cost by the reduction of the PGM loading required for the LNT and elimination of the urea injection for the SCR system [7]. The overall NOx conversion is still mostly confined in the LNT, which decreases at high temperatures (>400 C) due to deceased NOx storage capacity and NH$_3$ yield. A new LNT + active SCR system with urea dosing was proposed by researchers from SwRI [8] and Hyundai [9]. It uses a LNT to

* Corresponding authors. Tel.: +1 713 743 4322; fax: +1 713 743 432.
E-mail addresses: mharold@uh.edu (M.P. Harold), dluss@uh.edu (D. Luss).

overcome the SCR cold-start NOx emission, when the temperature is too low for urea dosing. The combined system has been demonstrated to meet the LEV III limits. It is a promising solution for LEV III-compliant diesel vehicles [10].

In contrast to the stand-alone urea-SCR system designed to operate with a lean exhaust, the combined LNT + SCR is inevitably exposed to a rich exhaust condition during the LNT regeneration. Deep rich purges are preferred to promote $NH_3$ generation by the LNT. This may generate relatively high levels of CO, $H_2$ and HC slippage to the SCR catalyst [11,12]. A recently-commercialized SCR on-filter (SCRF) technology comprises a diesel particulate filter (DPF) that is coated with SCR catalyst and is positioned in close proximity to the engine to enable fast SCR light-off. The SCR component encounters a rich environment during the periodic DPF regeneration events [13]. Even the SCR-only system may be exposed to a rich feed under certain conditions such as cold-start period, extended vehicle idling, engine malfunction, or degraded upstream diesel oxidation catalysts (DOC) [14,15]. All of these scenarios raise questions regarding the potential impact of rich reducing agents on the performance of the SCR catalyst.

Previous studies of the impact of various reductants on $NH_3$-SCR performance over metal-exchanged zeolites have mainly focused on HC species poisoning. It is well known that stored HC on zeolites can have a detrimental effect on both the SCR catalyst performance and its durability [16]. He et al. reported a negative effect of $C_3H_6$ due to carbon deposits during standard SCR (NO + $NH_3$ + $O_2$) over a Fe-beta zeolite [17]. Heo et al. attributed the competitive adsorption of $NH_3$ and $C_3H_6$ on the catalyst as well as undesired $NH_3$ consumption by side reactions to the decreased $NH_3$-SCR activities of Fe- or Cu-ZSM-5 [18]. Epling et al. compared the effects of $C_3H_6$ and dodecane (n-$C_{12}H_{26}$) exposure over two Cu-exchanged zeolite catalysts; one was a small-pore zeolite (Chabazite framework, CHA) while the second was a standard large-pore Cu-BEA zeolite [19]. The Cu-CHA had a much better resistance to HC poisoning than the Cu-BEA by effectively suppressing HC adsorption and coke formation. A slightly decreased standard SCR activity was observed when adding $C_3H_6$ to the gas fed to the Cu-CHA [19]. This was attributed to formation of partial oxidation intermediates. In a follow-up study, Kumar et al. found that even a small-pore zeolite could store non-negligible amounts of carbonaceous deposits from either short- or long-chain HCs via an oxygen-dependent, thermally-activated storage process [15]. All the above studies were conducted with continuous exposure of the SCR catalysts to a HC. Wang et al. [20] and Kim et al. [21] reported that under lean/rich cyclic conditions, the enhanced cycle-averaged NOx conversion over a Cu-CHA catalyst by $C_3H_6$, was attributed to the mitigation of HC poisoning and HC-SCR reactions.

The factors accounting for the impact of HC on $NH_3$-SCR over SCR zeolite catalysts include competitive adsorption, undesired $NH_3$ consumption, formation of partially oxidized intermediates and operating conditions (continuous or cyclic). A clear elucidation requires a systematic analysis. However, to date only a few studies investigated the effects of other reducing regents like CO and $H_2$ on $NH_3$-SCR zeolite catalysts. Huang et al. studied the deactivation of Cu-zeolites by reductive hydrothermal aging [14]. They found that extended exposure to a CO/$H_2$ mixture at 650 °C resulted in permanent catalyst deactivation due to the sintering of $Cu^0$ from the reduction of isolated $Cu^{2+}$ cations. Exposure to $C_3H_6$ under the same conditions resulted in a reversible deactivation after coke removal. Smith et al. [22] recently reported that compared to $C_3H_6$, CO and $H_2$ had a negligible effect on the $NH_3$-SCR chemistry over an Fe-zeolite catalyst, with the main contribution being a slight promotion of $NO_2$ reduction to NO.

To the best of our knowledge, the effects of a reductant mixture containing CO, $H_2$ and $C_3H_6$ on the SCR performance of a small-pore Cu-chabazite catalyst under either steady-state or cyclic operations

have not been systematically studied. To this end, in this study we examine the effects of each reductant through temperature ramp, step-response and cyclic experiments. The results can help in the interpretation of $NH_3$-SCR on Cu-CHA catalysts when subjected to rich exhaust exposure.

## 2. Experimental

### 2.1. Catalyst

A Cu-SSZ-13 SCR catalyst having a CHA framework was provided by BASF (Iselin, NJ). The SCR sample had a cell density of 400 cpsi and an estimated washcoat loading of about 2.4 g/in$^3$ with ca. 2.5 wt.% Cu loading. For bench reactor evaluation, a core sample was prepared (D = 0.8 cm, L = 1.0 cm, 28 channels). Prior to the reactor tests, the catalyst was de-greened at 500 °C for 5 h in a feed mixture containing 5% $O_2$, 2.5% $H_2O$, 2% $CO_2$, and balance of Ar.

### 2.2. Temperature ramp experiments

The bench-scale reactor set-up comprised a gas supply, tubular monolith reactor, and analytical and data acquisition systems. Gas flow rates were controlled by mass flow controllers (MKS Inc.) before entering the inline static mixer. Water was fed by a syringe pump (ISCO Model 500D) and vaporized in a heated line. A LabTech interface controlled the switching valve and mass flow controllers for the feed streams. The monolith catalyst was wrapped with Fiberfrax® ceramic paper and inserted inside a quartz tube (40.6 cm long, 1.27 cm outer diameter) mounted in a tube furnace coupled to a temperature controller. The temperature inside the reactor was measured by two 0.5 mm type-K stainless steel sheathed thermocouples (Omega Engineering Inc.). One placed 0.5 cm in front of the monolith measured the feed temperature. The second measured the temperature in the middle of the center monolith channel. The gaseous effluent concentrations of NO, $NO_2$, $N_2O$, $NH_3$, CO, $CO_2$ and $H_2O$ were measured by a calibrated FT-IR spectrometer (Thermo-Nicolet, Nexus 470).

The SCR catalyst was exposed to a constant feed composition at 500 °C to establish a steady state before the temperature ramp experiments. The downward temperature ramp to 200 °C was conducted at a rate of −2 °C/min to minimize the complicating effect of $NH_4NO_3$ formation. The ramp rate was sufficiently slow to avoid thermal hysteresis effects and to obtain essentially steady-state results. [Comment: The downward ramp was found to be more effective in this regard than an upward ramp. For example, the $NO_2$ SCR reaction ($NO_2$ + $NH_3$) is hard to reach steady-state at low temperature (~200 °C) due to the gradual accumulation of $NH_4NO_3$ on the catalyst; this process deactivates the catalyst and makes it difficult to differentiate among the effects of different reducing agents.] In some experiments, a step-response method was employed in order to evaluate both the transient and long-term response to gas concentration changes.

The feed gas composition for the baseline $NH_3$-SCR reactions comprised 500 ppm $NH_3$ and 500 ppm NO for standard SCR (NO/NOx = 1; 4NO + 4$NH_3$ + $O_2$ → 4$N_2$ + 6$H_2O$), 250 ppm NO and $NO_2$ for fast SCR (NO/NOx = 0.5; NO + $NO_2$ + 2$NH_3$ → 2$N_2$ + 3$H_2O$) and 500 ppm $NO_2$ for slow SCR (NO/NOx = 0; 3$NO_2$ + 4$NH_3$ → 3.5$N_2$ + 6$H_2O$)), in 0% or 5% $O_2$ (as specified) in a carrier gas of 2.5% $H_2O$, 2% $CO_2$ and balance Ar, at a space velocity of 120,000 h$^{-1}$. A reductant feed of either 1% CO or 1% $H_2$ or 500 ppm $C_3H_6$ was introduced as specified. The amount of $C_3H_6$ (500 ppm) was lower than that of CO (1%) or $H_2$ (1%) on a total reductant basis (the amount of O species that can be consumed by reductants); i.e., 500 ppm $C_3H_6$ can consume
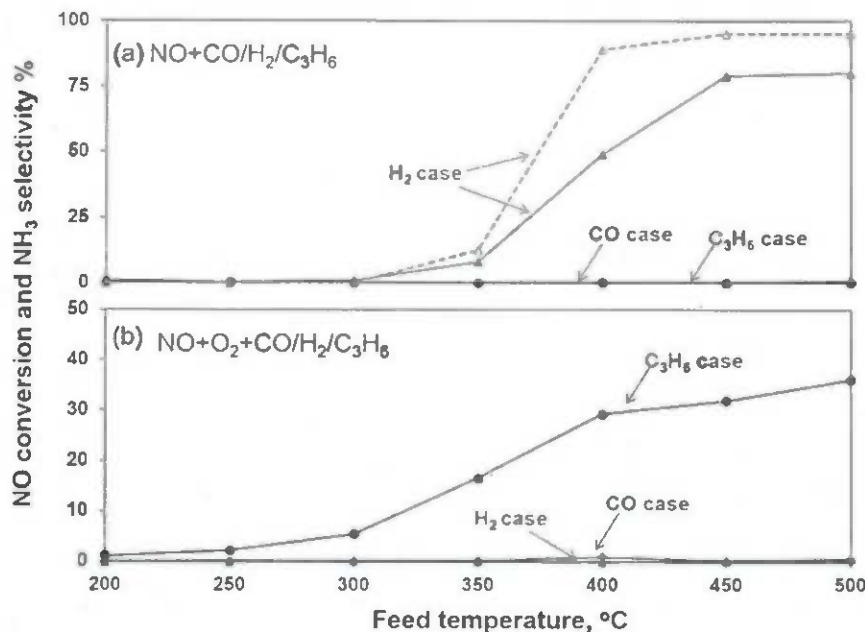
Fig. 1. NO conversion (solid) and NH₃ selectivity (dash) during reaction of NO (500 ppm) with three reductants (either 1% CO, 1% H₂, or 500 ppm C₃H₆) in the absence of O₂ (a) and in the presence of 5% O₂ (b).

4500 ppm O species, while 1% of either CO or H₂ can consume 1% O species.

### 2.3. Lean/rich cycling experiments

Lean/rich (30/5s) cycling experiments were conducted over the SCR catalyst. Table 1 describes the baseline cycling conditions. A reductant of either 1% CO or 1% H₂ or 500 ppm C₃H₆ was added to the baseline rich phase. The feed temperature was increased from 200 to 450 °C in steps of 50 °C. It typically took approximately ~10 min to reach a periodic steady state. At each temperature the cycle-averaged NOx (NO + NO₂) conversion for a particular operating condition was determined from the average of the final ten periodic cycles. The fractional NO$_x$ conversion was calculated by

$$X_{NO_x} = 1 - \frac{\int_0^{\tau_T} [F_{NO}(t) + F_{NO_2}(t)]\, dt}{\int_0^{\tau_T} [F^i_{NO}(t) + F^i_{NO_2}(t)]\, dt}$$

Here $\tau_T$ is the duration of a lean-rich cycle. $F^i_{NO}(t)$ and $F^i_{NO_2}(t)$ are the NO and NO₂ feed rates and $F_{NO}(t)$, $F_{NO_2}(t)$ are the effluent molar flow rates (mole/s).

### 2.4. Temperature-programmed desorption (TPD) experiments

Two types of TPD experiments were performed. The first evaluated the effects of the three reductants on the NH₃ storage capacity. The catalyst was exposed to 500 ppm NH₃ in a carrier gas with and without the presence of a reductant mixture containing 1% CO, 1%

**Table 1**
Gas condition for baseline cycling test.

| Gas | Lean (30 s) | Rich (5 s) |
| --- | --- | --- |
| NOx[a] | 300 ppm | 300 ppm |
| NH₃ | – | 500 ppm |
| O₂ | 5% | 1% |
| CO₂ | 2% | 2% |
| H₂O | 2.5% | 2.5% |

[a] NO/NOx = 1 for standard, 0.5 for fast and 0 for slow SCR reactions.

H₂ and 500 ppm C₃H₆ at 200 °C for 30 min, followed by another 30-min flush with carrier gas. The sample was then heated in carrier gas at a rate of 7.5 °C/min up to 500 °C. The second type studied the surface reactions between NH₄NO₃ and reducing agents. An equal amount of NH₄NO₃ was first loaded by co-feeding 500 ppm NH₃ and 500 ppm NO₂ to the SCR catalyst at 200 °C for 30 min, followed by a 30-min purge with carrier gas. The sample was then heated at 15 °C/min to 400 °C in a carrier gas (baseline), or in a mixture with either 1% CO or 1% H₂ or 500 ppm C₃H₆. Prior to each experiment, the catalyst was exposed to 5% O₂ in a carrier gas at 500 °C for 1 h.

## 3. Results and discussion

### 3.1. NO and NO₂ reactions with CO, H₂ and C₃H₆

Fig. 1 compares the NO conversion during the reaction of NO with CO, H₂ or C₃H₆ under both anaerobic and aerobic conditions. CO shows negligible NO conversion over the entire temperature range of 200–500 °C, regardless of the presence of O₂. Although C₃H₆ is inert to NO under anaerobic conditions, the presence of O₂ enables the reduction of NO to N₂ via a HC-SCR pathway, which involves propene partial oxidation intermediates to react with NO. On the other hand under anaerobic condition, H₂ begins to effectively reduce NO above 350 °C, with over 90% NH₃ selectivity. Copper-based catalysts have been reported to catalyze H₂-SCR reaction with metallic copper (Cu⁰) as the catalytically active site [23]. Cu-exchanged SSZ-13 is considered to contain isolated Cu cations as active centers. Thus, the first step in H₂-SCR by Cu-SSZ-13 likely involves the reduction of Cu ions to Cu⁰. H₂-TPR method has been widely utilized to assess the reducibility of various copper species on Cu-CHA catalysts. For example, H₂ is capable of reducing Cu ions like Cu-dimers to Cu⁰ at temperatures above ~350 °C [24], which coincides with the light-off temperature of NO reduction by H₂ in Fig. 1a. This supports the speculation of a stepwise mechanism involving Cu⁰ formation followed by NO hydrogenation to NH₃.

The addition of O₂ inhibits the reaction of NO with H₂ as seen in Fig. 1b. This is attributed to two factors. First, Cu⁰ catalyzes the
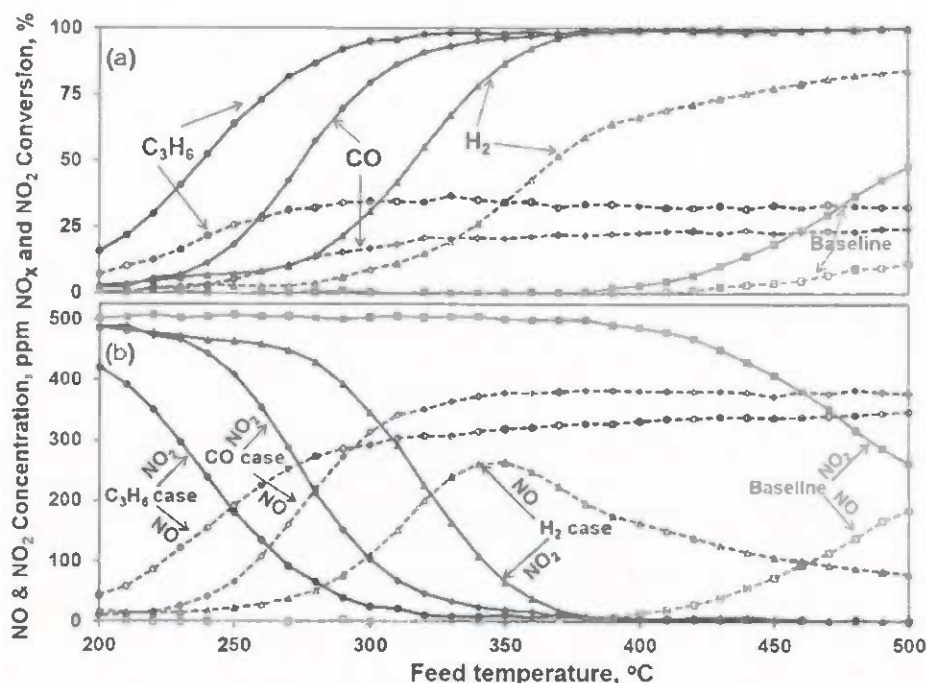
Fig. 2. (a) $NO_2$ (solid) and NOx (dash) conversion; (b) corresponding $NO_2$ (solid) and NO (dash) effluent concentration during reaction of $NO_2$ with three reductants (either 1% CO, 1% $H_2$, or 500 ppm $C_3H_6$) in the absence of $O_2$; Baseline condition: 500 ppm $NO_2$, 2.5% $H_2O$, 2% $CO_2$ in Ar.

oxidation of $H_2$ by $O_2$ which reduces the $H_2$ available for NO reduction. Second, the excess $O_2$ inhibits the formation of $Cu^0$ by oxidizing $Cu^0$ to either Cu cations or CuO cluster [14], both of which result in less $Cu^0$ available for NO adsorption and/or reduction.

Fig. 2a compares the $NO_2$ and NOx conversions over a wide temperature range during the reaction of $NO_2$ with CO, $H_2$ or $C_3H_6$ in the absence of $O_2$. Fig. 2b shows the corresponding effluent NO and $NO_2$ concentrations over the same temperature range. $C_3H_6$ exhibits the highest reactivity with $NO_2$, leading to the lowest light-off temperature (defined here as the temperature at which NOx conversion is 50% of the maximum). $NO_2$ reduction by $C_3H_6$ begins at 200 °C and increases up to ~300 °C where it levels off at 100% $NO_2$ conversion and ~35% NOx conversion. CO starts to reduce $NO_2$ at ~225 °C and plateaus at 100% $NO_2$ conversion and ~23% NOx conversion at 350 °C. Although $NO_2$ reduction by $H_2$ is the least effective on the basis of having the highest light-off temperature, the NOx conversion increases up to ~85% at 500 °C, in contrast to the plateaus observed for $C_3H_6$ and CO.

The NO and $NO_2$ effluent concentrations shown in Fig. 2b provide additional insights into the reactions of $NO_2$ with CO, $H_2$ or $C_3H_6$. $NO_2$ reduction to NO promoted by either CO or $C_3H_6$ occurs with concomitant and near-stoichiometric formation of NO. This is seen clearly at low temperatures; i.e., moles $NO_2$ consumed are equal to the moles NO produced. Both $C_3H_6$- and CO-assisted $NO_2$ conversion begin at 200 °C and reach 100% $NO_2$ conversion above 350 °C. It is worth noting that the N-balance is not closed at high temperatures in the baseline case. This is most likely due to the formation of some undetected gaseous $HNO_3$ that leaves the reactor.

The reaction of $NO_2$ with $C_3H_6$ was previously reported as part of the following HC-SCR pathway:

$$NO_{2(ad)} + C_3H_6 \rightarrow R\text{-}NO_2 \tag{R1}$$

$$R\text{-}NO_2 \rightarrow C_xH_yO_z + NO \tag{R2}$$

$$NO_{2(ad)} + C_3H_6 \rightarrow C_xH_yO_z + NO \qquad (R3 = R1 + R2)$$

$$C_xH_yO_z + NO_2/(NO + O_2) \rightarrow CO_2 + N_2 + H_2O \tag{R4}$$

The overall HC-SCR reaction is given by:

$$C_3H_6 + 9/2NO_2 \rightarrow 3CO_2 + 3H_2O + 9/4N_2 \tag{R5}$$

Gorce et al. [25] proposed that organic nitro intermediates (denoted by $R\text{-}NO_2$) formed by the reaction of $C_3H_6$ and ad-NOx species (R1), decompose to NO and oxygenates ($C_xH_yO_z$, such as acrolein) (R2). In turn, the oxygenates serve as active intermediates that further react with $NO_2$ or $NO + O_2$ to proceed the HC-SCR pathway (R4).

Overall reaction (R3) accounts for the stoichiometric conversion of $NO_2$ to NO. It also explains the appearance of the plateau in the NOx conversion for $C_3H_6$ in Fig. 2a, which coincides with the complete conversion of $NO_2$. That is, a lack of $NO_2$, which is required for reaction with oxygenates (R4), limits further NOx conversion and results in the plateau.

We propose the following nitrate-related mechanism for CO:

$$2NO_2 + O^{2-} \leftrightarrow NO_3^- + NO_2^- \tag{R6}$$

$$CO + NO_3^- \rightarrow NO_2^- + CO_2 \tag{R7}$$

$$NO_2^- + NO_2 \leftrightarrow NO + NO_3^- \tag{R8}$$

The overall reaction (R7 + R8) is given by

$$CO + NO_2 \rightarrow NO + CO_2 \tag{R9}$$

Nitrates formed by $NO_2$ disproportionation (R6) are reduced to nitrites by CO (R7), followed by their rapid reaction with $NO_2$, generating NO (R8). This reaction pathway was verified in a separate experiment when pulsing CO to the SCR catalyst initially contacted with $NO_2$ for 1 h at 300 °C (data not shown here). The instantaneous $CO_2$ release upon the feed of CO confirms the reactivity between nitrates and CO. This is discussed further below. Forzatti et al. [26] proposed a similar reduction of nitrates over a LNT catalyst by CO to form nitrites with evolution of $CO_2$.

Compared to CO and $C_3H_6$, $H_2$ is not as effective in the reduction of $NO_2$ to NO. For example, 95% $NO_2$ conversion is achieved at ~380 °C, somewhat higher than that for $C_3H_6$ (~300 °C) and CO
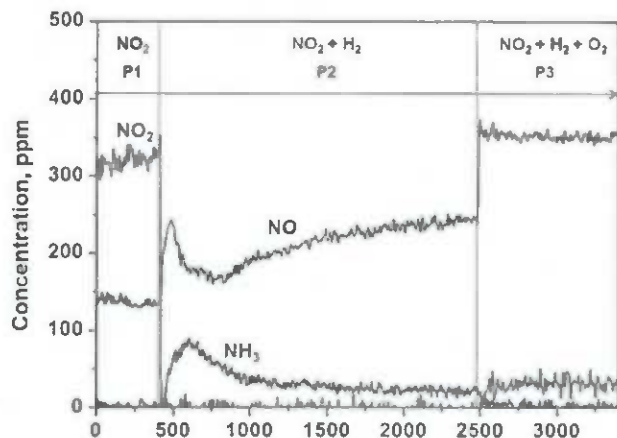
Fig. 3. Effluent species concentrations during a three-phase step-response protocol at 500 °C: (500 ppm $NO_2$, 1% $H_2$, 5% $O_2$ if required, in carrier gas of 2.5% $H_2O$, 2% $CO_2$ and balance Ar).



Fig. 4. $NH_3$-TPD profiles after saturating the catalyst with $NH_3$ at 200 °C in the absence (baseline) or in the presence of a mixture of reductants, including 1% CO, 1% $H_2$, and 500 ppm $C_3H_6$.

(~350 °C). Note that a peak in the effluent NO concentration occurs at ~350 °C. The increasing NO concentration to the left of the peak is likely due to a similar $NO_2$ reduction pathway as for CO, with $H_2$ reducing nitrates to nitrites (R10) that can further reduce $NO_2$ to NO (R8). This reaction pathway was verified by introducing $H_2$ to a pre-nitrated SCR catalyst at 300 °C. The nearly instantaneous production of $H_2O$, $NO_2$ and NO at the moment of $H_2$ admission agrees with the following proposed nitrate-related pathway.

$$H_2 + NO_3^- \rightarrow NO_2^- + H_2O \qquad (R10)$$

$$NO_2^- + NO_2 \leftrightarrow NO + NO_3^- \qquad (R8)$$

The decreasing NO concentration above 350 °C, at which point the $H_2$-SCR of NO begins to light off as shown in Fig. 1a, is attributed to increased $H_2$-SCR activity. Based on the established mechanism for $H_2$-SCR, which involve the adsorption and dissociation of $H_2$ and NOx over metallic metal sites [27], we expect that the following $H_2$-SCR pathway is favored over the above nitrate-related pathway at higher temperature range:

$$Cu^{2+} + H_2 \rightarrow Cu^0 + 2H^+ \qquad (R11)$$

$$H_2 + 2Cu^0 \rightarrow 2H\text{-}Cu^0 \qquad (R12)$$

$$NO_2 + 2Cu^0 \rightarrow NO\text{-}Cu^0 + O\text{-}Cu^0 \qquad (R13)$$

$$NO + 2Cu^0 \rightarrow N\text{-}Cu^0 + O\text{-}Cu^0 \qquad (R14)$$

$$N\text{-}Cu^0 + 3H\text{-}Cu^0 \rightarrow NH_3 + 4Cu^0 \qquad (R15)$$

$$2N\text{-}Cu^0 \rightarrow N_2 + 2Cu^0 \qquad (R16)$$

To examine the above pathways, a three-phase step response protocol was employed. As shown in Fig. 3, the protocol consisted of a $NO_2$ feed (500 ppm $NO_2$, Phase 1), followed by the addition of 1% $H_2$ in the absence (Phase 2) and presence (Phase 3) of 5% $O_2$ at 500 °C. During the Phase 1, $NO_2$ undergoes the thermal decomposition, producing NO. A sharp decrease in $NO_2$ concentration to nil with a corresponding steep increase in NO concentration occurs upon the introduction of $H_2$ in Phase 2. The NO rapidly peaks and then decreases to a local minima at ~250 s entering Phase 2, followed by a gradual increase up to the 2450 s mark. The NO peak is attributed to the rapid reduction of accumulated surface nitrates to nitrites (R10) that then reduce $NO_2$ to NO (R8). Meanwhile, the formation of metallic copper sites which catalyze the $H_2$-SCR reaction, reduces the NOx to $N_2$ and $NH_3$ (R11-16). The prolonged $H_2$ exposure results in a sintering of metallic copper that is responsible for a gradual decrease in NO conversion from 750 to 2450 s. Huang et al.
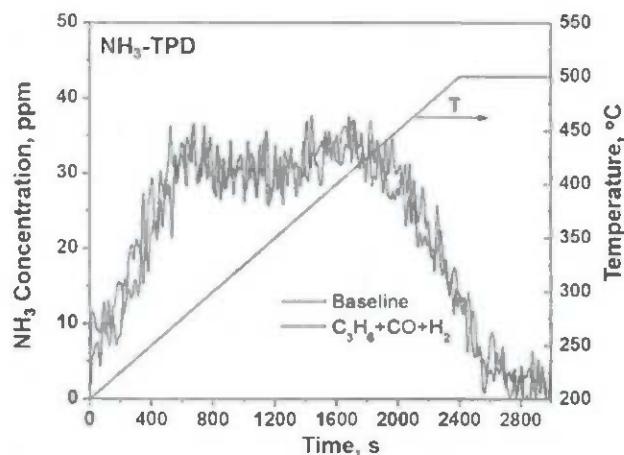
[14] reported that a high-temperature reducing treatment of Cu-zeolite catalysts by $H_2$ caused an irreversible sintering of Cu metals and thus the catalyst deactivation. Subsequent $O_2$ introduction in Phase 3, leads to a sharp increase in NO concentration. This confirms that the presence of $O_2$ inhibits $H_2$-SCR reaction as was shown by in Fig. 1b. In addition, $NO_2$ disproportionation (R6) is favored by the presence of $O_2$ to produce nitrates for the nitrate-related pathway. The inhibition of $H_2$-SCR pathway and the promotion of the alternative nitrate pathway results in a higher NO level under aerobic conditions.

### 3.2. The effects of CO, $H_2$ and $C_3H_6$ on $NH_3$ oxidation and storage

$NH_3$ storage plays a crucial role in the $NH_3$-SCR performance, especially at low temperatures. Thus, it is important to assess the effects of reducing agents on the $NH_3$ storage. Heo et al. reported that $C_3H_6$ competes with $NH_3$ for storage sites over Cu-ZSM-5, leading to inhibiting NOx reduction [18]. Epling et al. reported negligible $C_3H_6$ adsorption on Cu-SAPO-34 under anaerobic conditions, indicating that $C_3H_6$ may not compete with $NH_3$ for adsorption on the active sites [19]. Kumar et al. showed that extended exposure of Cu-SAPO-34 to $C_3H_6$ in the presence of $O_2$ at temperatures between 200 and 400 °C deceased $NH_3$ storage capacity. This is attributed to the formation of carbonaceous deposits which block the storage sites [15]. Wang et al. reported the co-adsorption of $C_3H_6$ and $NH_3$ on Cu-SSZ-13 under anaerobic conditions with no apparent coupling between the two adsorbates [20]. Finally, no studies of the effect of CO or $H_2$ on $NH_3$ storage on Cu-CHA have been reported. Since $H_2$ and CO are considered as effective molecular probes in the characterization of various copper species over Cu-zeolite catalysts; i.e., $H_2$ can reduce the oxidation state of Cu ions, while CO can strongly adsorb onto $Cu^+$ to form carbonyls [28], these may affect the $NH_3$ adsorption on Cu cations.

Fig. 4 shows $NH_3$ TPD profiles on Cu-SSZ-13 after being saturated at 200 °C with $NH_3$ in the presence and absence of CO, $H_2$ and $C_3H_6$. Two desorption peaks, one at ~275 °C and the second at ~400 °C, were observed during the temperature ramp; these can be assigned to $NH_3$ adsorbed on weak acid sites (Cu cation or extra-framework Al Lewis sites) and stronger acid sites (Brønsted sites), respectively [29]. The near overlap of the two $NH_3$ desorption profiles indicates that addition of CO, $H_2$ and $C_3H_6$ has a negligible impact on both $NH_3$ storage capacity and the strength of different acid sites. These data suggests that none of the three reductants competes with $NH_3$ for the acid storage sites of the Cu-chabazite catalyst.

# DOCKET ALARM

# Explore Litigation Insights

Docket Alarm provides insights to develop a more informed litigation strategy and the peace of mind of knowing you're on top of things.

## Real-Time Litigation Alerts

Keep your litigation team up-to-date with **real-time alerts** and advanced team management tools built for the enterprise, all while greatly reducing PACER spend.

Our comprehensive service means we can handle Federal, State, and Administrative courts across the country.

## Advanced Docket Research

With over 230 million records, Docket Alarm's cloud-native docket research platform finds what other services can't. Coverage includes Federal, State, plus PTAB, TTAB, ITC and NLRB decisions, all in one place.

Identify arguments that have been successful in the past with full text, pinpoint searching. Link to case law cited within any court document via Fastcase.

## Analytics At Your Fingertips

Learn what happened the last time a particular judge, opposing counsel or company faced cases similar to yours.

Advanced out-of-the-box PTAB and TTAB analytics are always at your fingertips.

## API

Docket Alarm offers a powerful API (application programming interface) to developers that want to integrate case filings into their apps.

### LAW FIRMS
Build custom dashboards for your attorneys and clients with live data direct from the court.

Automate many repetitive legal tasks like conflict checks, document management, and marketing.

### FINANCIAL INSTITUTIONS
Litigation and bankruptcy checks for companies and debtors.

### E-DISCOVERY AND LEGAL VENDORS
Sync your system to PACER to automate legal marketing.